OPEN ACCESS
JOURNAL OF ADVANCED DIELECTRICS
Vol. 12, No. 3 (2022) 2250006 (10 pages)

DOI: 10.1142/S2010135X22500060

Modeling the effect of uniform and nonuniform dispersion of nanofillers on electrical tree propagation in polyethylene dielectric

Khola Azhar* and Salman Amin
Electrical Engineering Department, University of Engineering and Technology, Taxila, Punjab 47080, Pakistan
*khola.azhar25@gmail.com

Received 4 January 2022; Revised 10 April 2022; Accepted 28 April 2022; Published 15 June 2022

A phase-field model is developed in this paper based on the similarity between mechanical fracture and dielectric breakdown. Electrical treeing is associated with the dielectric breakdown in solid dielectrics by the application of high voltages. Instead of explicitly tracing the propagation of conductive channel, this model initializes a continuous phase field to characterize the extent of damage. So far, limited research has been conducted for simulating the effect of nanofiller dispersion on electrical treeing. No study has modeled the effect of uniform and nonuniform dispersion of nanofillers with varying filler concentration on treeing. Since electrical treeing tends to decrease the breakdown strength of solid dielectrics therefore, nanofillers are widely used to distract the tree from a straight channel to distribute its energy in multiple paths. Diverting a straight treeing channel into multiple paths reduces the chances of its propagation from live to dead-end hence, improving the breakdown strength. The physical and chemical nature of nanofillers has a crucial impact on increasing the resistance to treeing. In this paper, phase-field model is developed and used to simulate electrical treeing in polyethylene for varying concentrations of alumina nanofiller using COMSOL Multiphysics. Tree inception time, tree-growth patterns, and corresponding changes in dielectric strength is studied for both dispersions. Electrical treeing under different concentrations of alumina nanofillers with uniform and nonuniform dispersion is investigated in polyethylene as a base material. It is observed that fillers with uniform dispersion increases the resistance to treeing and tree inception time. Highest resistance to treeing is observed by adding 1% nanoalumina uniformly in raw polyethylene. Moreover, in uniform dispersion the tree deflects into multiple branches earlier than nonuniform dispersion impeding the damage speed as well.

Keywords: Phase-field model; dielectric breakdown; resistance to treeing; uniform and nonuniform filler dispersion.

Abbreviations

HVDM : High-voltage dielectric material
PFM : Phase-field model
PE : Polyethylene
PVDF : Polyvinyledene fluoride
XLPE : Cross-linked polyethylene
TIT : Tree initiation time
PDE : Partial differential equation
PD : Partial discharge.

1. Introduction

Solid dielectrics experience irreversible degradation phenomena, which leads to the complete failure of insulation material. When solid dielectrics are subjected to high electric stresses, electrical treeing starts which is basically a degradation phenomenon in solids. From these treeing paths, partial discharge (PD) begins and therefore, the tree propagates in the direction of the applied electric field. Once the tree reaches the opposite electrode, the insulation is bridged and can never be recovered hence, it is called an irreversible breakdown. In high-voltage dielectric materials (HVDMs), electrical treeing often occurs as a precursor of dielectric breakdown phenomena.[1–4] To develop reliable insulations for power industries and other applications, it is required to study the insight of electrical treeing mechanisms and find ways to suppress treeing. The tree originates from the point where the electric field is highly concentrated such as a sharp edge or a void defect.[5] Electric field localization is usually caused by defects (voids and contaminants) which may be present in the insulation at the time of manufacturing or afterward due to electromechanical stress and chemical pollutants present in the environment.[1]

Treeing phenomena have three significant phases i.e., tree initiation, propagation, and extinction.[6] Researchers identified so many factors that control the tree growth which are applied voltage, frequency, temperature, nonuniform or concentrated electric field, and PD.[7–9] In general, the electrical tree initiation is greatly influenced by the magnitude, polarity,[10] and type of voltage (AC,[11] DC, and impulse). Also the effect of bipolar square wave voltage,[12] distributed DC waveform,[13] ramp voltage,[14] harmonics,[15] and superimposed DC voltage[16] on electrical treeing growth was studied. Under relatively high applied voltages,[17] temperature[18,19] or frequencies[20,21] electrical tree becomes fractal. Electrical treeing in base material Perspex,[22] epoxy,[23] cross-linked polyethylene

*Corresponding author.

(XLPE),[24,25] and under the effect of alumina filler,[26] ZnO filler,[27] MgO filler,[28] and SiO_2 filler[29,30] was also investigated. In the past few years, several models have been proposed for understanding the electrical treeing mechanism.[1,31] Different methods have also been adopted to enhance the dielectric strength such as adding inorganic nanofillers into the dielectric which divides the breakdown channel into multiple paths and increases the resistance to treeing.[32–39] A branched breakdown path (multiple paths) can dissipate more energy than a single channel therefore, by dividing a straight channel into multiple paths the dielectric strength can also be enhanced.[40]

1.1. *Existing models on electrical treeing*

There are two different common approaches to model electrical treeing. The first is statistical, and the second is a physics-based approach. The statistical models use various statistical techniques to illustrate the breakdown of solid dielectrics by fitting the data collected from experiments to statistical distributions, i.e., Weibull distribution,[41] log-normal distribution,[42] and Johnson SB distribution.[43] The physics-based models include physical mechanisms like the dielectric breakdown model,[44,45] the discharge-avalanche model,[46] and the field-driven tree-growth model.[47] Table 1 briefly describes the existing models.

These models give an insight into treeing mechanism. Recently a phase-field model (PFM) was used to simulate the breakdown in nanocomposite polyvinylidene fluoride (PVDF) and $BaTiO_3$,[49] inspired by the similarity between dielectric breakdown and brittle fracture.[17,50–53] Another study used PFM to simulate electrical treeing with needle-shaped fillers.[54] Moreover, the influence of nanoparticle on treeing in epoxy is also studied.[55] PFM was also used to investigate dielectric breakdown in ferroelectric polymers,[56] and ceramics.[57]

No study has modeled the effect of uniform and nonuniform dispersion for varying filler concentrations on electrical treeing. This study investigates the effect of both dispersions on electrical treeing. In the proposed research, PFM is used to simulate the initiation and propagation of electrical treeing in polyethylene (PE) and investigate the effect of both dispersions on suppressing electrical tree for various concentrations of alumina nanofiller. This paper presents fundamental modeling concepts, phase-field formulations, and how they interpret the physical phenomena. COMSOL implementation strategy, dimensions of loading geometry, and various other specifications have been discussed. Obtained numerical results for three cases (treeing in raw PE, under the effect of nonuniformly, and uniformly dispersed alumina nanofillers) have been presented and thoroughly discussed for varying filler concentrations. Further, it contains the basic comparison between the treeing propagation under all the three cases mentioned above. Finally, the conclusion summarizes the outcome of this work and potential future recommendations.

Table 1. Classification of models for simulating electrical treeing propagation through solid dielectrics.[48]

	Physical	Empirical	Deterministic	Stochastic	Multiphysical	Cellular automata
Introduction and methodology:	In this model, a physical experiment is carried out involving electrical aging and dielectric breakdown. Based on the results a model or equation is developed.	Use analytical expressions attained by the curve-fitting method in experimental results.	It is based on electrostatics and local electron avalanches to model the PD within the tree structure.	Electrical stress is calculated repeatedly at the point of interest, considering treeing as an iterative process.	Describing treeing phenomena into algebraic equations, and then post-processing the data.	Widely used for modeling complex systems. It divides solid dielectric into a matrix of cells to investigate treeing and its various aspects.
Conclusion:	The physical model is sometimes difficult to build due to lack of resources.	There is a linear correlation between the fractal dimension and the time required for breakdown.	Damage caused by treeing is directly proportional to energy dissipated in PD.	Discrete growth and propagation probability usually rely on the magnitude of the local electric field strength.	Propagation of plasma channels depends on ionization processes as well as electromechanical and electrothermal instabilities.	Dielectric breakdown is considered discrete in time and space and can be analyzed by using local interactions.
Application:	Useful for quantitative investigation of the dependence between tree propagation and applied voltage.	Can be used to find a relationship between time and length during tree propagation.	Branched trees can be obtained without random variables, as fluctuations in the electric field strength are controlled by PD.	Helpful to predict the effect of barriers on electrical tree growth.	Predict the useful life of dielectric as a function of the applied voltage, temperature, and fractal dimension with a single equation.	Used to examine the effect of space charge carriers on tree propagation.

The aim of this paper is to model the effect of uniform and nonuniform filler dispersion on electrical treeing, and an attempt to delay the breakdown process in solid dielectrics.

2. Phase-Field Model for Electrical Treeing

Phase-field formulations and methodology are discussed in this section. Figure 1 shows the workflow for the development of PFM to simulate electrical treeing. Once the model is developed and the electrical tree is simulated, then we can investigate various other properties by analyzing the effect of uniform and nonuniform dispersion for various concentrations of nanofiller.

The simulation of electrical treeing is followed by the similarity between mechanical fracture and dielectric breakdown. The detailed modeling is discussed in Refs. 49 and 53. A scalar field is something that has a value at each point in space and time. It is required to initiate a phase-field variable "$d(x, t)$" which can predict the permittivity change for different phases (intact phase, damaged phase, partial damaged phase). A scalar phase-field "$d(x, t)$" is initialized which is both spatial and time-dependent where variable "d" is used to describe the damage status of dielectric. The value of "d" will determine the severity of the damage which is ranging between (0 and 1). If $d = 1$, the material is healthy indicating that there is no damage or treeing whereas for $d = 0$, the material is fully damaged. For any intermediate state when the material is partially damaged, "d" takes any value between 0 and 1. The noticeable fact is that the material has now a state-dependent permittivity $\varepsilon(d)$ indicated in equations $1(a–c)$ for healthy, partially damaged, and fully damaged state:

Equation (1(a)) indicates the permittivity for undamaged material.

for $d = 1$:

$$\varepsilon_{\text{intact}} = \varepsilon_0, \tag{1a}$$

ε_0: Initial permittivity for intact material.

Equation (1(b)) indicates the permittivity for intermediate damage state.

for $0 < d < 1$:

$$\varepsilon_{\text{partially damaged}} = \frac{\varepsilon_0}{f(d)+\lambda} \tag{1b}$$

(interpolated by $f(d) = 4d^3 - 3d^4$).[53]

Equation (1(c)) indicates the permittivity for a fully damaged state.

for $d = 0$:

$$\varepsilon_{\text{fully damaged}} = \frac{\varepsilon_0}{\lambda}, \tag{1c}$$

where "λ" is usually a small number that determines the permittivity of the damaged zone, for example if $\lambda = 1\times10^{-3}$ it means the permittivity in damaged region will be 1000 times than that of the intact region. However, "λ" should not be too small so that the permittivity of the damaged region becomes infinite. As the conductivity of damaged region increases consequently, the tree propagates with very high speed making the system highly dynamic. This makes it difficult for the software to converge the solution.[53] However keeping "λ" sufficiently small by applying ramping and other such techniques could resolve the issue of high dynamics and ill convergence. During electrical treeing, material damage takes place which decreases the total potential energy of the system. The total energy of the system "Π" can be computed by considering the combined effect of three forms of energies by evaluating the volume integral, as indicated in Eq. (2)

$$\Pi[d,\phi] = \int_{\Omega}\left[W_{\text{es}}(E,d) + W_d(d) + W_i(\nabla d)\right]dV \tag{2}$$

where

Ω: Spatial domain occupied by the solid dielectric,

ϕ: Electrode potential.

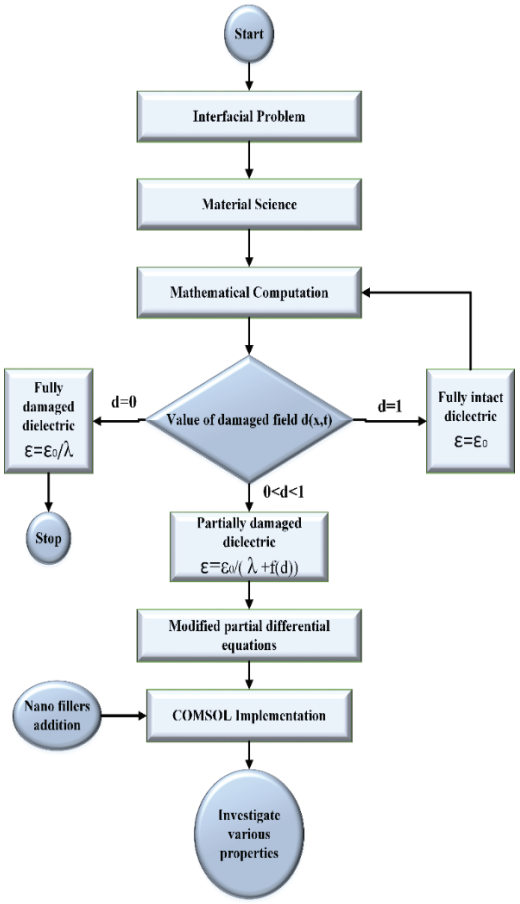

Fig. 1. Workflow for simulating electrical tree by PFM.

Moreover, the electric potential "$\phi(x, t)$" is related to electric field "$E = -\nabla\phi$".

The expressions for these three forms of energies are expressed in Eqs. (3)–(5).

1. W_{es} complementary electrostatic energy per unit volume:

$$W_{es}(E,d) = \frac{-\varepsilon}{2} E \cdot E. \tag{3}$$

2. W_d damage energy:

$$W_d(d) = W_c\left[1 - f(d)\right], \tag{4}$$

where W_c is the critical density of electrostatic energy.

3. $W_i(\nabla d)$ Gradient energy term:

$$W_i(\nabla d) = \frac{\Gamma}{4} \nabla d \cdot \nabla d. \tag{5}$$

It is the interface energy, use to regulate sharp phase boundaries where Γ is approximately the breakdown energy.

2.1. *Linear kinetics law*

The proportionality between the rate of damage and energetic driving forces enables us to employ the linear kinetic law indicated in Eq. (6).

$$\frac{\partial d}{\partial t} = -\mu \frac{\delta \Pi}{\delta d}. \tag{6}$$

Here, "μ" is the mobility that is a material parameter, and it determines the speed of damage in the dielectric.

Substituting the three forms of energy function in linear kinetic law, and expressing as the summation of electrostatic, damage and interface contribution in Eq. (7):

$$\frac{1}{\mu}\frac{\partial d}{\partial t} = \frac{\varepsilon'(d)}{2} \nabla\phi \cdot \nabla\phi + W_c f'(d) + \frac{\Gamma}{2} \nabla^2 d. \tag{7}$$

For modeling, we normalize the above equations to get the principal dimensionless equations for simulating electrical tree patterns in COMSOL. The requirement of several material parameters that are often difficult to find can be reduced by normalization. Energy density (W_{es}) is normalized by W_c, time (t) by $\frac{1}{\mu W_c}$, electric potential (ϕ) by $\sqrt{\Gamma/\varepsilon_0}$, and length ($l$) by $\sqrt{\Gamma/W_c}$.

Following are the PFM equations that describe the physics of the treeing phenomena:

$$\bar{\nabla}.\left(\frac{1}{f(d)+\lambda}\overline{\nabla\phi}\right) = 0, \tag{8}$$

$$\frac{\partial d}{\partial \bar{t}} = -\frac{f'(d)}{2\left[f(d)+\lambda\right]^2}\overline{\nabla\phi}.\overline{\nabla\phi} + f'(d) + \frac{1}{2}\bar{\nabla}^2 d. \tag{9}$$

In Eqs. (8) and (9), the over-bar symbols are dimensionless quantities. The simulations are performed by loading both these equations along with other parameters in a two-dimensional (2D) domain using COMSOL Multiphysics. The study is time-dependent due to the presence of time-dependent derivatives. Along with proper initial and boundary conditions, the geometry is loaded, and these equations are computed for two fields $\bar{\phi}(\bar{x},\bar{t})$ and $d(\bar{x},\bar{t})$. To introduce randomness in the simulation for the initiation of the electrical tree, we introduce a random function and add this perturbation with the coefficient of damage energy term in the equation representing the rate of damage.[49]

3. Results and Discussion

The loading setup is a rectangle-shaped specimen and voltage is applied across the electrodes through boundary conditions as shown in Fig. 2. Voltage is applied by controlling the charge accumulation (Q=It) of the lower electrode. In numerical calculations, a dimensionless discharge speed (I_d) is considered (normalizing I by $\mu\Gamma\sqrt{\varepsilon_0 Wc}$), which can be changed by changing either mobility "μ" or controlling electric current "I". The material is homogenous, so we introduce some randomness into it as discussed previously.

As seen from Fig. 2, this sample is twice in length as compared to width. A field concentrator of length 1/10 times the total length is placed at the center of the upper boundary because the breakdown process or treeing usually initiates from the points where the field is concentrated. Therefore, at the tip of this conductive line, the field is concentrated enough to initiate electrical treeing and propagates toward the ground electrode.

3.1. *Electrical tree initiation and propagation*

Figures 3(a)–3(d) show the initiation and propagation of the electrical tree for a specified time-lapse. The shading

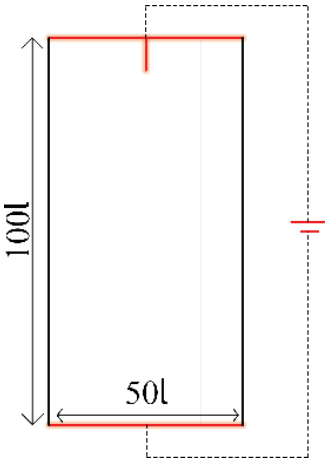

Fig. 2. Loading setup schematic.

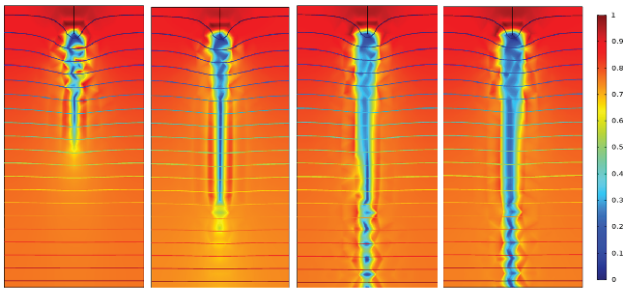

Fig. 3. (Color Online) (a)–(d) tree initiation and propagation for different time steps, the blue color represents the damage whereas the red represents no damage. The contour lines are equipotential lines for the electric field (a) for the time around 0.5 S, (b), (c) for the time about 0.6 S, and (d) for 0.63 S, all time steps have different potential and damage is increasing with the potential.

represents damage variable "*d*" in which the damaged region is indicated in blue, and the healthy region is shown in red, the other shades represent partially damaged dielectric. The contour lines represent the electric potential. The tree growth shown in Figs. 3(a)–3(d) is for successive time steps.

Effect of varying concentration of nanofiller on electrical breakdown:

The effect of the addition of nanofiller on electrical treeing under uniform and nonuniform dispersion with varying percentages is investigated independently and presented for each case in the subsequent sections.

To make the dispersion of nanofiller according to a specific percentage, first, the area of specimen is calculated and then the number of required nanofillers (to cover a specific percentage of the total area) is estimated. These nanofillers are then placed in the simulated model of specimen uniformly and nonuniformly. More number of nanofiller particles are required in order to increase the filler concentration.

3.2. *Tree suppression by nonuniform dispersion of nanofiller*

Electrical treeing has three different phases i.e., inception, propagation, and extinction. The last phase will lead to complete dielectric breakdown. In this section, the nonuniform dispersion of nanofillers with varying filler concentrations from 0.2% to 1% is presented. The treeing initiation in nonuniform dispersion of nanofiller starts after 0.6 s compared to 0.5 s in the raw dielectric. As more energy is dissipated in multiple paths rather than the single channel therefore, additional energy will be required for complete dielectric breakdown. Nanofiller distracts and divides the tree into multiple paths, so tree inception time (TIT) is increased. The nanofiller attracts the treeing channel toward itself due to its permittivity. Consequently, electrical tree propagates slowly in a branched channel (multiple branches) via high resistance path, rather than a straight low resistance path.

Figures 4–8 are for varying filler concentrations and each is presented for four different time stages (a)–(d). When the filler concentration is low, the breakdown path is slightly tilted as shown in the last two stages of Figs. 4–6. For higher filler concentration, the channel tries to divide into multiple paths as shown in the last two stages of Figs. 7 and 8. From Figs. 4(a)–4(d) and 5(a)–5(d) (corresponding to 0.2% and 0.4% filler concentrations), we see that by the addition of nanofiller the treeing channel is slightly tilted due to surface energy of the nanofiller. As the concentration of nanofiller increases in Figs. 6(a)–6(d) (corresponding to 0.6% filler concentration), a second channel tries to begin at the bottom. In Figs. 7(a)–7(d) and 8(a)–8(d) (corresponding to 0.8% and 1% filler concentrations), it can be seen clearly that for the later stages ((c) and (d)) the treeing tries to form multiple channels as compared to initial stages ((a) and (b)). This happens at the cost of increasing filler concentration as in Figs. 7 and 8, and at later stages. Initiation of multiple paths at an earlier stage with lower filler concentration further improves the dielectric strength. Any conclusion made about the effectiveness of nanofiller in tree suppression by nonuniform dispersion is not as much reliable as compared to their uniform

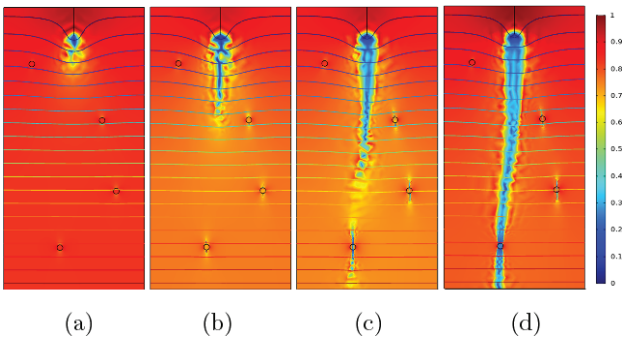

Fig. 4. (a)–(d): 0.2% nonuniform filler dispersion for different time steps.

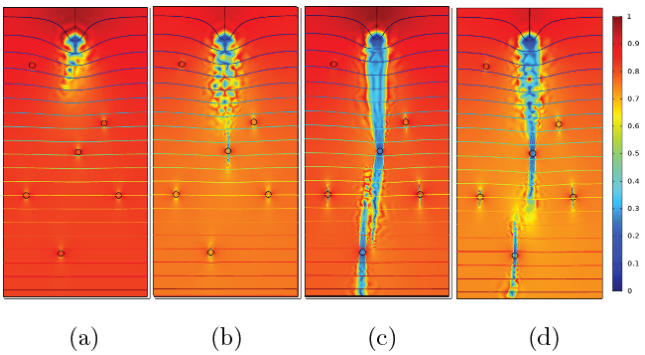

Fig. 5. (a)–(d): 0.4% nonuniform filler dispersion for different time steps.

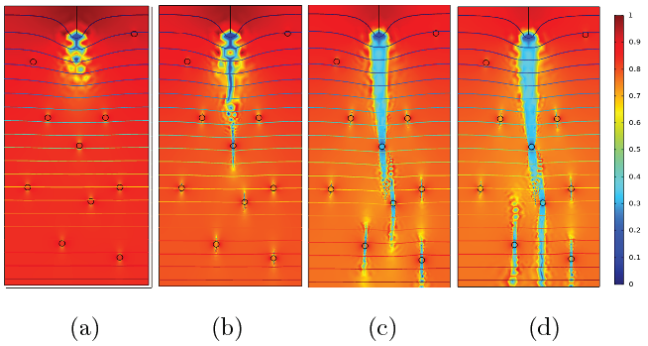

Fig. 6. (a)–(d): 0.6% Nonuniform filler dispersion for different time steps.

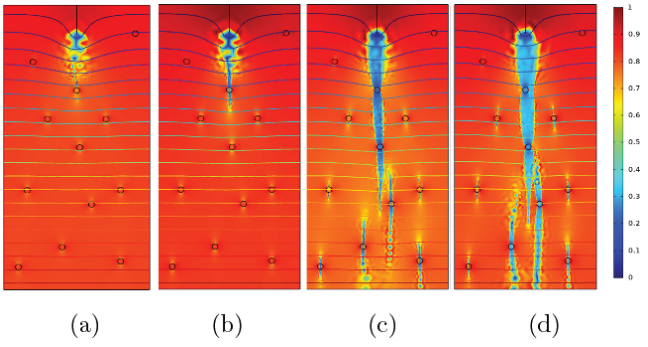

Fig. 7. (a)–(d): 0.8% Nonuniform filler dispersion for different time steps.

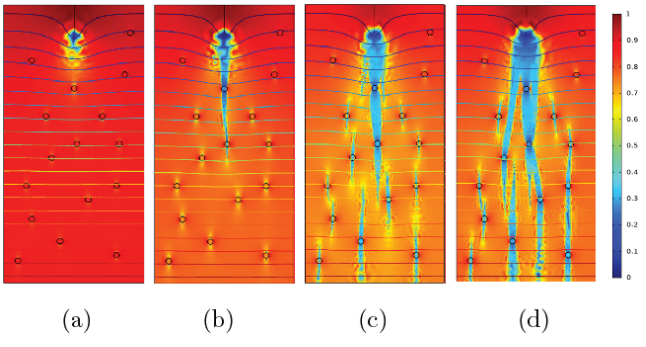

Fig. 8. (a)–(d): 1% nonuniform filler dispersion for different time steps.

dispersion. In the next section, uniform dispersion for various percentages of fillers is presented.

3.3. *Tree suppression by uniform dispersion of nanofiller*

Fortunately, while simulating with COMSOL we can arrange the nanofillers uniformly (at a specified distance) which is a limitation in the practical approach. Instead of nonuniformly dispersing the nanofillers as in the previous section, here we uniformly arrange them to develop a uniform electric field which will delay the breakdown. The TIT for uniform dispersion of nanofiller is around 0.8 s (for 1% filler concentration, respectively). In uniform dispersion, branching of the channel occurs earlier and even with low filler concentration. This is due to conduction between neighboring filler particles that are symmetrically dispersed.

Comparing Figs. 3(a)–3(d)–8(a)–8(d) with Figs. 9(a)–9(d)–13(a)–13(d), we observe that TIT has been increased as treeing becomes slow. In previous cases, the tree initiates between 0.5 and 0.67 s but now after uniformly distributing nanofillers, the tree initiates at about 0.75–0.8 s. In Figs. 10(a)–10(d) (corresponding to 0.4% uniform filler concentration) six nanofillers are placed symmetrically. Till Fig. 10(b) the tree has one path. As it propagates further, the conductive breakdown channel splits due to surface energy of nanofiller. Therefore, channel divides itself as shown in Fig. 10(c). In Figs. 11(a)–11(d) (corresponding to 0.6% uniform filler concentration), ten nanofillers are placed symmetrically. As compared to Figs. 10(b) and 10(c), we can see that Figs. 11(b) and 11(c) have dual channels sideways and some minor channels try to form in between. It increases the resistance to treeing which improves the breakdown strength. Similarly in Figs. 12(a)–12(d) (corresponding to 0.8% uniform filler concentration), 12 nanofillers are placed symmetrically. The improvement in results can be seen by comparing the treeing

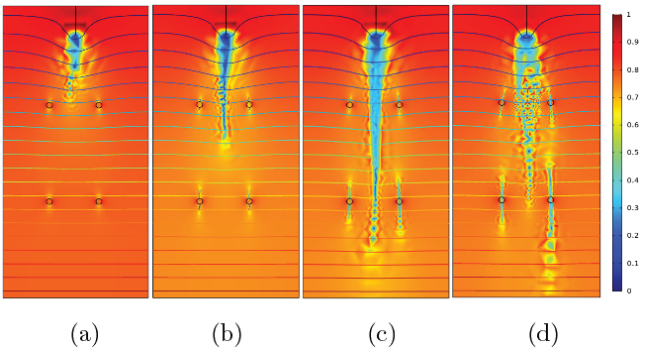

Fig. 9. (a)–(d): 0.2% Uniform filler dispersion for different time steps.

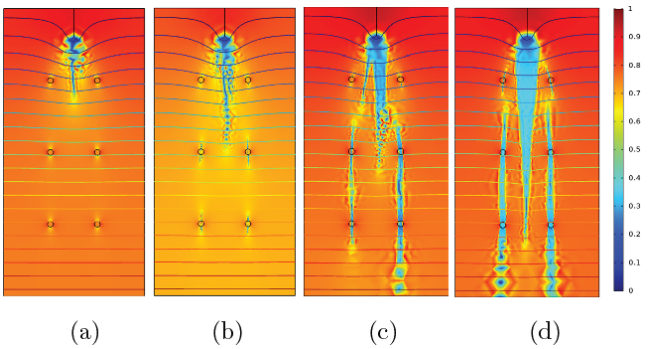

Fig. 10. (a)–(d): 0.4% uniform filler dispersion for different time steps.

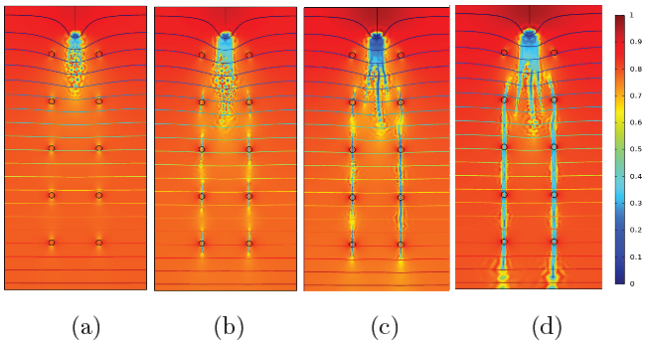

Fig. 11. (a)–(d): 0.6% uniform filler dispersion for different time steps.

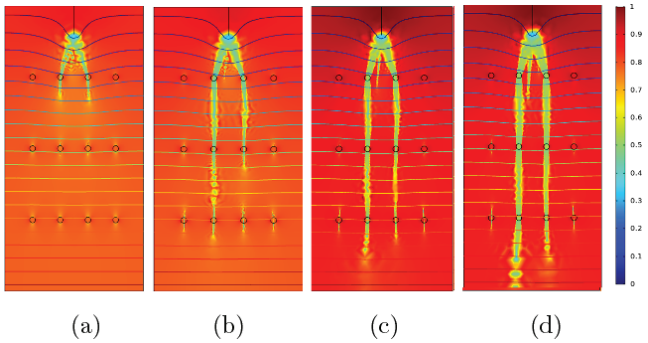

Fig. 12. (a)–(d): 0.8% Uniform filler dispersion for different time steps.

pattern in Figs. 9(a), 10(a), and 11(a) with Fig. 12(a). It is obvious that for the same time step, the tree divides into two channels as in Fig. 12(a) than in previous cases shown in Figs. 9(a), 10(a), and 11(a). As shown in Figs. 13(a)–13(d) (corresponding to 1% uniform filler concentration), 16 nanofillers are placed symmetrically. It is clear from Figs. 13(a) and 13(b) the tree divides into three channels earlier than ever before. In all the uniform dispersion cases, the treeing has become slow as it tries to have more than one path. Moreover, the branching of the channel in uniform dispersion is more obvious as compared to the multiple channels formed in nonuniform dispersion.

By looking at the treeing patterns, it is clear that tree branching into multiple paths is dissipating more energy hence, resulting in breakdown strength improvement. When the filler attracts the channel, the tree is inherently divided into more than one path which will impart higher resistance to treeing and results in dielectric strength improvement. Above 1% filler concentration the tree is again propagating speedily, it does not divide into branches quickly as in the case of Fig. 13(a). Damage will occur above 1% filler concentration because some conductivity is introduced in the dielectric by the addition of filler particles, after a specific filler concentration the dielectric properties slightly shift toward conduction and this is why the

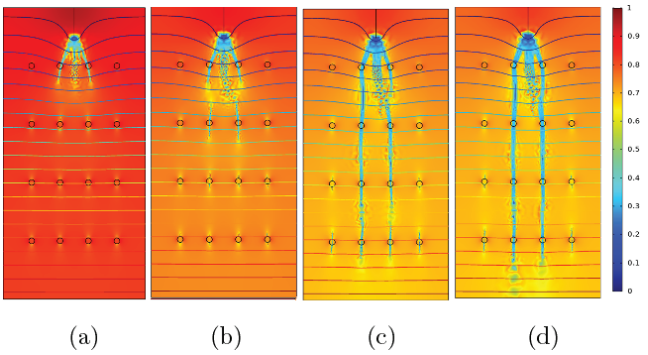

Fig. 13. (a)–(d): 1% uniform filler dispersion for different time steps.

treeing is relatively fast above 1% filler concentration, also reducing the dielectric strength. Therefore at 1% uniformly dispersed alumina filler, the dielectric shows superior performance. Whereas, below and above 1% the dielectric is damaged earlier.

The effect of uniform and nonuniform dispersion of alumina fillers in PE base for varying concentrations on electrical treeing is summarized in Table 2. In this table, the highest breakdown strength has been reported at 1% alumina filler in PE, above 1% filler concentration the breakdown strength is again relatively low. The possible reason for this behavior is the uniformity which is created in the electric field and introduces semi-conductive effect in the dielectric. Increasing the filler concentration produces the extra alignment above 1% filler loading consequently, it lowers the dielectric strength. Since all the loadings >1% impart nearly the same effect on breakdown strength i.e., lowering the strength therefore, the last row presents the overall effect for >1% filler loadings.

Figure 14 shows the speed of electrical tree propagation under all three conditions (uniformly/nonuniformly filled and unfilled dielectric).

4. Comparison of Electrical Treeing Patterns

The damage state of the dielectric at a fixed applied voltage in each of the three cases (i.e., raw, uniform, and nonuniform dispersion of filler), is investigated with varying nanofiller concentrations. It can be seen in Fig. 15(a) for raw dielectric that the breakdown constitutes a greater region. Bulk of the material is damaged as shown in the blue area, also the treeing reaches 100% of the sample length. In Fig. 15(b) for nonuniform dispersion, the dielectric strength is relatively improved as the tree length has been reduced to almost 70% of sample length for the same applied voltage and time. In Fig. 15(c) for uniform dispersion, the dielectric strength is greatly enhanced and resistance to treeing also increases, the tree does not propagate more than 50% of sample length. Furthermore, the single channel has been divided into multiple paths enabling it to dissipate more energy. Now

Table 2. Effect of Various Concentrations of Fillers (Uniformly and Nonuniformly Dispersed) on the Electrical Treeing, Nominal Breakdown Strength, and TIT for $\varepsilon_{filler} = 9.3$ (Alumina) and $\varepsilon_{base} = 2.2$ (PE).

Raw dielectric				Nonuniform dispersion			Uniform dispersion		
Nominal breakdown strength	TIT (s)	Resistance to treeing	Filler %age	Nominal breakdown strength	TIT (s)	Resistance to treeing	Nominal breakdown strength	TIT (s)	Resistance to treeing
0.89	0.5371	Low	0.2%	1.05	0.63705	Low	1.16	0.75624	Low
			0.4%	1.07	0.65218	Low	1.17	0.77238	Low
			0.6%	1.08	0.67055	Low	1.18	0.78334	Low
			0.8%	1.08	0.67058	Medium	1.19	0.7900	Medium
			1%	**1.09**	**0.67060**	**High**	**1.23**	**0.80901**	**High**
			>1%	1.06	0.67000	Low	1.15	0.78123	Low

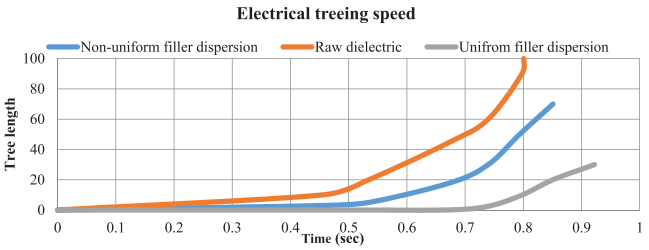

Fig. 14. Comparison of electrical treeing speed by a line graph, for raw PE and PE with 1% alumina filler under uniform and nonuniform dispersion, TIT verses tree in sample of length 100l.

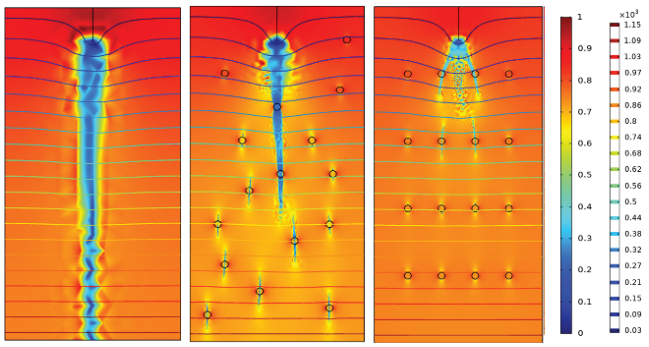

Fig. 15. (a)–(c) Comparing the effect of unfilled and filled (uniform and nonuniform) dielectric on treeing pattern at fixed applied voltage (a) treeing pattern in raw dielectric without any filler. (b) treeing pattern with 1% nonuniformly dispersed alumina nanofillers. (c) treeing pattern with 1% uniformly dispersed alumina nanofillers. The legend represents electric potential "ϕ" and damage variable "d".

additional time and voltage are required for tree propagation, therefore, increasing TIT. Hence uniform dispersion of nanofillers could improve the dielectric strength more than nonuniform dispersion.

Previous research studies were carried out without considering the method of filler dispersion for various concentrations.[49,53,58] Despite the results reported in earlier studies, the effect of filler dispersion is not completely understood yet. However, filler dispersion has a crucial role in setting up the electric field which is responsible for the dielectric breakdown. Therefore, a better understanding of filler dispersion is the requisite for the development of innovative HVDMs. The proposed PFM investigates the effectiveness of the filler dispersion method for various concentrations of filler in suppressing electrical tree. The treeing pattern shows the improvement in the dielectric strength under both uniform and nonuniform dispersions.

5. Conclusion

Investigation of electrical treeing in the laboratory requires a lot of time and resources. Electrical treeing, a type of dielectric breakdown, is studied by the PFM approach in this paper, transforming the complex physical phenomena into a couple of partial differential equations in which every variable has a physical meaning. To improve the dielectric strength, the effect of adding alumina nanofillers (uniformly and nonuniformly dispersed) was examined. Treeing phenomena in pure PE and PE alumina nanocomposite were investigated with varying filler concentrations. It was observed that the addition of 1% by weight of alumina nanofiller (uniformly dispersed) improves the resistance to treeing of the dielectric. The effect of fillers dispersion on electrical tree propagation is interpreted by using PFM.

Nonuniform dispersion of nanofillers improves the breakdown strength up to 22.4% whereas the uniform dispersion of nanofillers improves up to 38.2%. Nonuniform electric field is a mandatory condition for dielectric breakdown. Under uniform dispersion, the electric field mostly remains uniform and less intensified therefore, the breakdown phenomena is suppressed. The TIT is increased from 0.5 s in the raw dielectric to 0.80 s with uniform dispersion of 1% alumina nanofillers, also tree extinction time increased appreciably. Treeing patterns observed in this study illustrate that by uniformly

distributing the nanofillers, one can delay the electrical tree successfully. Hence, such dielectrics could be possibly used for any extra-high-voltage applications. Practically, it is difficult to set the exact location of filler into the dielectric but phase-field modeling enables us to distribute the fillers at the desired location and percentage using COMSOL. This research paper also sets the basis for further studies such as the effect of different filler's permittivity, geometries, and sizes on treeing to understand electrical treeing phenomena with more depth in other composite dielectrics.

References

[1]M. H. Ahmad *et al*., An overview of electrical tree growth in solid insulating material with emphasis of influencing factors, mathematical models and tree suppression, *TELKOMNIKA Indones. J. Electr. Eng.* **12**, 5827 (2014).

[2]L. A. Dissado, Understanding electrical trees in solids: From experiment to theory, *IEEE Trans. Dielectr. Electr. Insul.* **9**, 483 (2002).

[3]H. Mcdonald, Ageing in epoxy resin as a precursor to electrical treeing, Ph.D. thesis, The University of Manchester, UK (2020).

[4]C. S. K. Abdulah *et al*., Electrical tree investigation on solid insulation for high voltage applications, *2021 IEEE Symp. Industrial Electronics & Applications (ISIEA)* (IEEE, 2021), pp. 1–6.

[5]N. Shimizu and C. Laurent, Electrical tree initiation, *IEEE Trans. Dielectr. Electr. Insul.* **5**, 651 (1998).

[6]A. L. Barclay and G. C. Stevens, Statistical and fractal characteristics of simulated electrical tree growth, *1992., Sixth Int. Conf. Dielectric Materials, Measurements and Applications* (IET, 1992), pp. 17–20.

[7]Y. Zhou *et al*., Morphology of electrical trees in silicon rubber, *J. Electrostat.* **71**, 440 (2013).

[8]A. S. Vaughan, S. J. Dodd and S. J. Sutton, A Raman microprobe study of electrical treeing in polyethylene, *J. Mater. Sci.* **39**, 181 (2004).

[9]C. R. A. Kumar *et al*., Investigation into the failure of XLPE cables due to electrical treeing: A physico chemical approach, *Polym. Test* **22**, 313 (2003).

[10]S. Kumara, T. Hammarström and Y. V. Serdyuk, Polarity effect on electric tree inception in HVDC cable insulation, *IEEE Trans. Dielectr. Electr. Insul.* **28**, 1819 (2021).

[11]G. M. Sahoo *et al*., Analysis of electrical tree growth in crossed link polyethylene cable insulation under different AC voltages, *2020 IEEE 9th Power India Int. Conf. (PIICON)* (IEEE, 2020), pp. 1–5.

[12]C. Zhang *et al*., Effect of bipolar square wave voltage with varied frequencies on electrical tree growth in epoxy resin, *IEEE Trans. Dielectr. Electr. Insul.* **28**, 806 (2021).

[13]T. Hammarström and S. M. Gubanski, Detection of electrical tree formation in XLPE insulation through applying disturbed DC waveforms, *IEEE Trans. Dielectr. Electr. Insul.* **28**, 1669 (2021).

[14]F. Esterl *et al*., Electrical treeing and partial discharges in DC-XLPE under constant DC voltage and repetitive DC ramp voltage, *VDE High Voltage Technology 2020; ETG-Symp*. (VDE, 2020), pp. 1–8.

[15]B. X. Du *et al*., Effects of harmonic component on electrical tree in EPDM for HVDC cable accessories insulation, *IEEE Trans. Dielectr. Electr. Insul.* **28**, 578 (2021).

[16]L. Zhu and H. Li, Effect of harmonic superimposed DC voltage on electrical tree characteristics in XLPE, *IEEE Trans. Appl. Supercond.* **31**, 1 (2021).

[17]J. V. Champion and S. J. Dodd, The effect of voltage and material age on the electrical tree growth and breakdown characteristics of epoxy resins, *J. Phys. D, Appl. Phys.* **28**, 398 (1995).

[18]Y. Zhang *et al*., Electrical treeing behaviors in silicone rubber under an impulse voltage considering high temperature, *Plasma Sci. Technol.* **20**, 54012 (2018).

[19]B. X. Du *et al*., Effect of ambient temperature on electrical treeing characteristics in silicone rubber, *IEEE Trans. Dielectr. Electr. Insul.* **18**, 401 (2011).

[20]Q. Nie *et al*., Effect of frequency on electrical tree characteristics in silicone rubber, *2009 IEEE 9th Int. Conf. Properties and Applications of Dielectric Materials* (IEEE, 2009), pp. 513–516.

[21]G. Chen and C. H. Tham, Electrical treeing characteristics in XLPE power cable insulation in frequency range between 20 and 500 Hz, *IEEE Trans. Dielectr. Electr. Insul.* **16**, 179 (2009).

[22]M Abderrahman, Investigation of electrical treeing in perspex material, *Appl. Res. Smart Technol.* **2**, 1 (2021).

[23]S. Chen *et al*., The importance of particle dispersion in electrical treeing and breakdown in nano-filled epoxy resin, *Int. J. Electr. Power Energy Syst.* **129**, 106838 (2021).

[24]N. S. Mansor *et al*., Study on the dielectric performance of XLPE nanocomposite against the electrical tree propagation, *2020 Int. Symp. Electrical Insulating Materials (ISEIM)* (IEEE, 2020), pp. 375–378.

[25]S. Chandrasekar, S. Purushotham and G. C. Montanari, Investigation of electrical tree growth characteristics in XLPE nanocomposites, *IEEE Trans. Dielectr. Electr. Insul.* **27**, 558 (2020).

[26]T. J. Mohamed, S. R. Faraj and H. K. Judran, Electrical treeing behavior in XLPE insulation due to content AL2O3 nanoparticles, *J. Phys., Conf. Ser.* Vol. 1973, No. 1, 12010 (2021).

[27]N. S. Mansor *et al*., Effect of ZnO nanofiller in the XLPE matrix on electrical tree characteristics, *IEEE Access* **8**, 117574 (2020).

[28]X. Zhu *et al*., Characteristics of partial discharge and AC electrical tree in XLPE and MgO/XLPE nanocomposites, *IEEE Trans. Dielectr. Electr. Insul.* **27**, 450 (2020).

[29]S. Chen *et al*., Electrical tree growth in microsilica-filled epoxy resin, *IEEE Trans. Dielectr. Electr. Insul.* **27**, 820 (2020).

[30]C. Kalaivanan and S. Chandrasekar, A study on the influence of SiO_2 nano particles on the failure of XLPE underground cables due to electrical treeing, *J. Electr. Eng. Technol.* **14**, 2447 (2019).

[31]Y. Nyanteh *et al*., Overview of simulation models for partial discharge and electrical treeing to determine feasibility for estimation of remaining life of machine insulation systems, *2011 Electrical Insulation Conf. (EIC)* (IEEE, 2011), pp. 327–332.

[32]J. C. Pandey and N. Gupta, Study of treeing in epoxy-alumina nanocomposites using electroluminescence, *IEEE Trans. Dielectr. Electr. Insul.* **26**, 648 (2019).

[33]T. Imai *et al*., Influence of temperature on mechanical and insulation properties of epoxy-layered silicate nanocomposite, *IEEE Trans. Dielectr. Electr. Insul.* **13**, 445 (2006).

[34]Y. Chen *et al*., Tree initiation phenomena in nanostructured epoxy composites, *IEEE Trans. Dielectr. Electr. Insul.* **17**, 1509 (2010).

[35]S. Raetzke *et al*., Tree initiation characteristics of epoxy resin and epoxy/clay nanocomoposite, *IEEE Trans. Dielectr. Electr. Insul.* **16**, 1473 (2009).

[36]C. Nyamupangedengu and D. R. Cornish, Time-evolution phenomena of electrical tree partial discharges in magnesia, silica and alumina epoxy nanocomposites, *IEEE Trans. Dielectr. Electr. Insul.* **23**, 85 (2016).

[37]W. Wang and Y. Yang, The synergistic effects of the micro and nano particles in micro-nano composites on enhancing the resistance to electrical tree degradation, *Sci. Rep.* **7**, 1 (2017).

[38]S. Alapati and M. J. Thomas, Electrical treeing and the associated PD characteristics in LDPE nanocomposites, *IEEE Trans. Dielectr. Electr. Insul.* **19**, 697 (2012).

[39]J. Wu *et al*., Characteristics of initial trees of 30 to 60 μm length in epoxy/silica nanocomposite, *IEEE Trans. Dielectr. Electr. Insul.* **19**, 312 (2012).
[40]X. Zhang *et al*., Giant energy density and improved discharge efficiency of solution-processed polymer nanocomposites for dielectric energy storage, *Adv. Mater.* **28**, 2055 (2016).
[41]A. L. Barclay *et al*., Stochastic modelling of electrical treeing: Fractal and statistical characteristics, *J. Phys. D, Appl. Phys.* **23**, 1536 (1990).
[42]H. J. Wiesmann and H.R. Zeller, A fractal model of dielectric breakdown and prebreakdown in solid dielectrics, *J. Appl. Phys.* **60**, 1770 (1986).
[43]H. R. Zeller, Breakdown and prebreakdown phenomena in solid dielectrics, *IEEE Trans. Electr. Insul.* Volume: EI-22, 115–122, Issue: 2, (1987).
[44]T. Farr, R. Vogelsang and K. Frohlich, A new deterministic model for tree growth in polymers with barriers, *2001 Annual Report Conf. Electrical Insulation and Dielectric Phenomena (Cat. No. 01CH37225)* (IEEE, 2001), pp. 673–676.
[45]G. Bahder *et al*., Physical model of electric aging and breakdown of extruded pplymeric insulated power cables, *IEEE Trans. Power Appar. Syst.* Volume: PAS-101, 1379–1390 (1982).
[46]L. A. Dissado and P. J. J. Sweeney, An analytical model for discharge generated breakdown structures, *[1992] Proc. 4th Int. Conf. Conduction and Breakdown in Solid Dielectrics* (IEEE, 1992), pp. 328–332.
[47]J. Champion, V, S. J. Dodd and G. C. Stevens, Analysis and modelling of electrical tree growth in synthetic resins over a wide range of stressing voltage, *J. Phys. D, Appl. Phys.* **27**, 1020 (1994).
[48]J. M. Rodríguez-Serna, R. Albarracín-Sánchez and I. Carrillo, An improved physical-stochastic model for simulating electrical tree propagation in solid polymeric dielectrics, *Polymers (Basel)* **12**, 1768 (2020).
[49]Z. Cai *et al*., Electrical treeing: A phase-field model, *Extreme Mech. Lett.* **28**, 87 (2019).
[50]F. Noto and N. Yoshimura, Voltage and frequency dependence of tree growth in polyethylene, *Conf. Electrical Insulation & Dielectric Phenomena-Annual Report 1974* (IEEE, 1974), pp. 207–217.
[51]S. J. Dodd, A deterministic model for the growth of non-conducting electrical tree structures, *J. Phys. D, Appl. Phys.* **36**, 129 (2002).
[52]M. Noskov *et al*., Computer simulation of discharge channel propagation in solid dielectric, *ICSD'01. Proc. 2001 IEEE 7th Int. Conf. Solid Dielectrics (Cat. No. 01CH37117)* (IEEE, 2001), pp. 465–468.
[53]W. Hong and K. C. Pitike, Modeling breakdown-resistant composite dielectrics, *Procedia IUTAM* **12**, 73 (2015).
[54]M.-X. Zhu *et al*., A phase field model for the propagation of electrical tree in nanocomposites, *IEEE Trans. Dielectr. Electr. Insul.* **27**, 336 (2020).
[55]P. Divya and P. Preetha, Influence of nanoparticles on electrical treeing in epoxy based dielectrics, *2021 IEEE Region 10 Symp. (TENSYMP)* (IEEE, 2021), pp. 1–5.
[56]Z. Mi *et al*., Phase field modeling of dielectric breakdown of ferroelectric polymers subjected to mechanical and electrical loadings, *Int. J. Solids Struct.* **217**, 123 (2021).
[57]Z. Cai *et al*., Dielectric breakdown behavior of ferroelectric ceramics: The role of pores, *J. Eur. Ceram. Soc.* **41**, 2533 (2021).
[58]K. Chaitanya Pitike and W. Hong, Phase-field model for dielectric breakdown in solids, *J. Appl. Phys.* **115**, 44101 (2014).